

# DAΦNE TRANSFER LINE FOR KLOE-2 PHYSICS RUN

A. De Santis, B. Buonomo, S. Cantarella, P. Ciuffetti, G. Di Pirro, A. Drago, L. Foggetta, A. Ghigo, C. Milardi, R. Ricci, U. Rotundo, M. Serio, A. Stecchi, A. Stella,  
Istituto Nazionale di Fisica Nucleare - Laboratori Nazionali di Frascati  
v. Enrico Fermi 40, 00044, Frascati (RM) Italy  
A. Michelotti, Consorzio Cabibbo-Lab, Rome, Italy.

## Abstract

The transfer lines of the DAΦNE accelerator complex have been revised and optimized in view of the forthcoming KLOE-2 physics run. The transfer lines consolidation activities involved low level systems, diagnostics tools and control system procedures dealing with polarity switch of the magnetic element during the injection. The work done determined a substantial improvement in the transfer lines stability and reproducibility, speeding up the polarity switch and increasing the injection efficiency thus achieving a considerable reduction of the background hitting the experimental detector during the process.

## INTRODUCTION

The Frascati electron-positron collider DAΦNE [1] began operations in 2001 delivering physics data to the KLOE experiment [2] and providing high K meson rates, at the energy of the  $\phi$  resonance, to three different experiments, which logged  $\sim 4.5 \text{ fb}^{-1}$  total integrated luminosity in dedicated physics runs. In the same period the collider performance has been constantly improved by several progressive upgrades and better machine understanding. The detailed study of the factors limiting the maximum achievable luminosity gave birth to the proposal for a different collision scheme based on large Piwinski angle and *Crab-Waist* (CW) compensation of the beam-beam interaction [3]. This novel approach has been implemented on DAΦNE [4] in a shut-down already planned during 2008 to install SIDDHARTA, a compact detector without axial magnetic field [5], offering a simplified environment to test the new configuration. With this new setup the instantaneous luminosity achieved was  $4.53 \times 10^{32} \text{ cm}^{-2} \text{ s}^{-1}$  peak value, corresponding to a factor of three higher than best performance obtained with previous setup, and with a maximum daily integrated luminosity of the order of  $\sim 15 \text{ pb}^{-1}$  [6, 7].

The achieved results lead the KLOE collaboration to present a project to upgrade the experimental apparatus in view of a new physics run [8]. KLOE-2 is a multipurpose experiment devoted, mainly, to study decays of K mesons as well as several hadronic physics and low energy quantum chromodynamics phenomena. The detector consists of a large cylindrical drift chamber (outer tracker),  $\sim 3.5 \text{ m}$  long and  $2 \text{ m}$  in radius, surrounded by a lead-scintillating fiber electromagnetic calorimeter. The interaction region is surrounded by a novel cylindrical GEM inner tracker. The experiment is fully inserted inside a superconducting coil providing axial magnetic field of  $0.52 \text{ T}$ . The two trackers (inner

and outer) performance as well as the trigger efficiency are strongly dependent on the machine background, especially during the injection.

The typical lifetime ( $\sim 10 \text{ min}$ ) observed during the SIDDHARTA run drives to continuous injection, which affects negatively the KLOE-2 physics run [9] introducing dead time in the trigger, up to 10%, and enhancing the machine background hitting the detector. These reasons pushed to a general review of the DAΦNE injection system.

The DAΦNE injection system consists of two Transfer Lines (TLs) driving the beam from the LINAC to the Main Rings (MRs) going through the Damping Ring (DR). The two TLs have common sections and are operated with different setup for electron and positron injections.

## UPGRADE ACTIVITIES

To achieve the target efficiency and reliability several interventions had to be realized.

### Cooling System

The cooling system of the TLs and DR has been revised and a new low level automatic control system developed in order to stabilize the temperatures of the magnetic elements making them independent of the daily thermal excursion. Currently the cooling plant of the entire DAΦNE complex is handled by a central supervisor system that reports alarms, faults and logs system-wide working parameters. Having an efficient supervising process helps to operate the accelerator complex and to schedule maintenance interventions.

### Control System

The control system of DAΦNE was largely revised for the KLOE-2 physics run [10]. The injection system is now driven by virtual machines operating via point-to-point TCP/IP connections. This simplified scheme allows faster switching procedure, halving the time needed to commute between electron and positron injection. This result has a relevant impact on the maximum instantaneous luminosity which usually is achieved when both beam currents have their highest values.

### Charge Measurement in TL

Nine integrating current transformer (ICTs), equipped with wall current bypass and electromagnetic shields, have been installed over ceramic gaps in the vacuum chamber along the TLs. Each ICT is capable of integrating the fast rise-time pulse induced by the LINAC (DR) beam with a 20

ns time constant and is connected through coaxial cables to an array of Bergoz BCM detection board electronics [11] whose pseudo-DC outputs, proportional to the pulse charge, are sampled by VME ADCs. Electron or positron pulse charges are acquired at the beam rate at each pickup, according to the different DAΦNE timing states associated with the transport of  $e^\pm$  pulses along different zones of the machine: **LSP** LINAC to spectrometer, **LBT** LINAC to BTF, **LTA** LINAC to DR **AMR** DR to MR, and displayed on the control system consoles. A dedicated storing process allows offline analysis, to provide evaluation of the injection efficiency useful for machine tuning and the charge integrals over time, required for radiation safety monitoring [12]. These data can be easily accessed via a dedicated web interface (DJANGO) shown in Fig. 1.

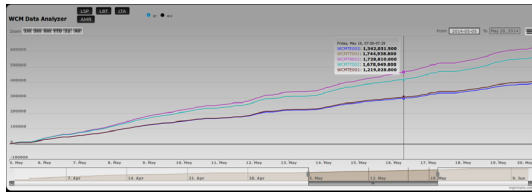


Figure 1: DJANGO web interface. Integrated currents in the period of May 2014 for the electron injection in AMR section.

### Orbit Measurement

The closed orbit in the DR is extracted from the beam position monitor (BPM) signals through a commercial digital receiver, then acquired and processed by a dedicated task integrated in the DAΦNE control system.

The eight button electrodes BPMs and four short circuited strip-lines BPMs installed along the ring, are multiplexed and sent to a Libera Brilliance board [13] where the RF signals are processed and down-sampled to 113.667 MHz. All data path provided by the board (slow acquisition, ADC raw, turn by turn) can be acquired via TCP/IP through the Libera generic server.

### DAMPING RING MEASUREMENTS

The magnetic lattice of DR is based on four quasi-achromatic arcs, each of them having two  $45^\circ$  bending magnets, three quadrupoles providing the needed focusing and two sextupoles for chromaticity correction. A total of eight corrector magnets (both horizontal and vertical) are installed in order to keep the orbit under control. Four septa and two pairs of fast electromagnetic kickers are used to inject and extract beams.

The DR has been designed and built according to the original DAΦNE project. Implementing the CW collision scheme determined a shortening of the MRs nominal orbit. In principle the DR should have been modified accordingly, since the DR RF frequency must be kept in the ratio 1/5 with respect to the MRs one. Therefore a shorter reference orbit was obtained reducing the bending radius of the DR dipoles

without any mechanical modification of the vacuum chamber. This has been possible due to the very large DR acceptance in the transverse plane. Therefore a detailed study of the new DR optics is recommended to improve the MR injection efficiency and quality. The DR modeling is based on MAD-X package [14] and in Fig. 2 the betatron functions calculated with the model are compared with the measurements.

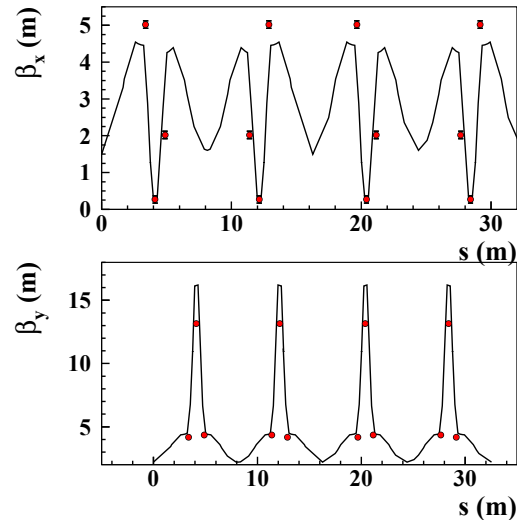


Figure 2: Comparison between computed (solid line) and measured (dots) horizontal (upper plot) and vertical (lower plot) betatron functions.

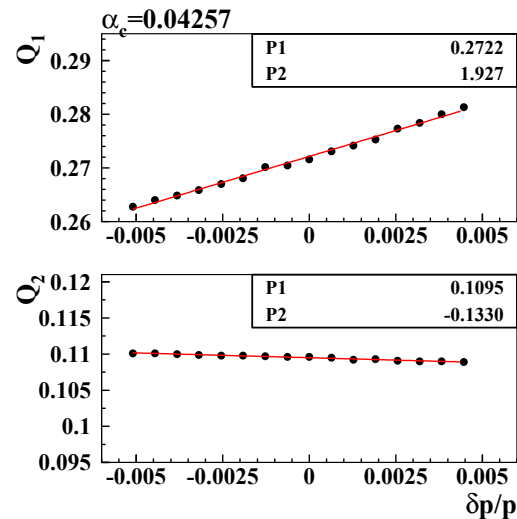


Figure 3: Horizontal (upper plot) and vertical (lower plot) chromaticity (dots) as a function of momentum variation. The red line is a fit with a linear function.

The chromaticity measured with tune variation as a function of relative momentum variation is shown in Fig. 3. Experimental data have been interpolated with a linear function  $Q_j = P_1 + P_2 \delta p/p$ . Higher order terms are measured with large correlation with the previous one even with the

Content from this work may be used under the terms of the CC BY 3.0 licence (© 2014). Any distribution of this work must maintain attribution to the author(s), title of the work, publisher, and DOI.

large span of momentum variation ( $\pm 0.5\%$ ) considered and then have been neglected. From this measurement the expected large energy acceptance of the DR is clearly confirmed.

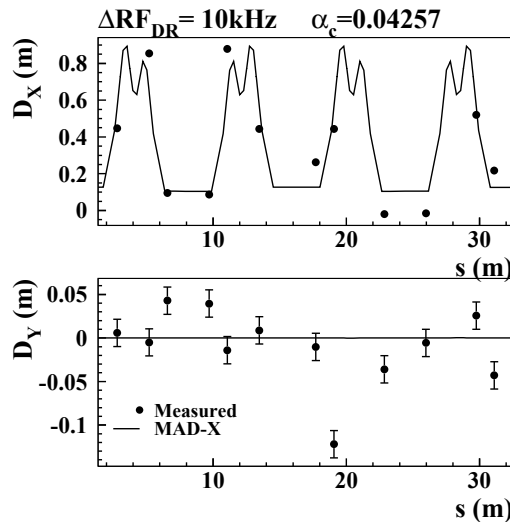


Figure 4: Comparison between horizontal (upper plot) and vertical (lower plot) dispersion calculated by the model (solid line) and measured by varying the RF frequency (dots). In the upper plot the error bars are inside experimental data. The momentum compaction factor ( $\alpha_c = 0.04257$ ) has been taken from the DR model.

By using the orbit acquisition tool several measurement has been performed: dispersion, alignment errors and corrector magnets response matrix. The dispersion function is shown in the Fig. 4.

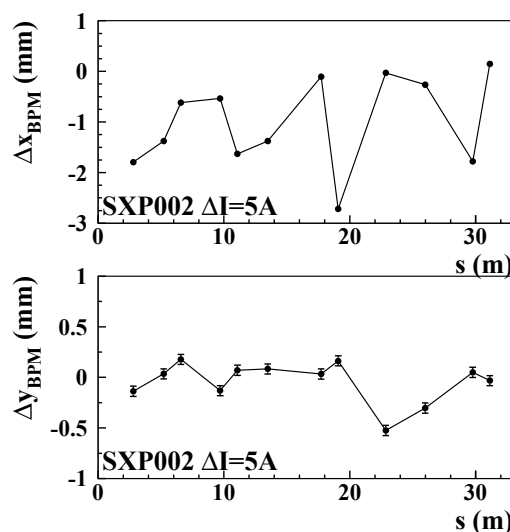


Figure 5: Orbit variation induced by sextupole current change of 5 A (set point 182 A). It is quite evident the effect of horizontal (upper panel) and vertical (lower panel) orbit displacements due to a magnet misalignment.

The agreement between measurement and model is not perfect, this is largely due to misalignment in the quadrupole and sextupole magnets along the ring as can be deduced from Fig. 5 presenting the orbit displacement due to a sextupole current variation of 3% w.r.t. its nominal setting.

A comparison between calculated and measured orbit displacement induced by a corrector magnet is reported in Fig. 6, in this case the calculated orbit variation matches quite well the experimental result despite the errors connected to the element misalignment.

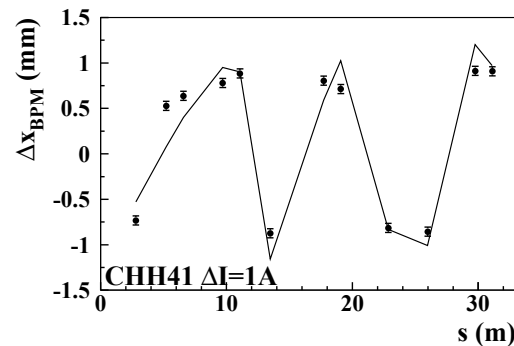


Figure 6: Comparison between calculated (solid line) and measured (dots) orbit displacement induced by varying the current of a horizontal corrector in the DR.

## CONCLUSIONS

The diagnostic tools of the DAΦNE injection system have been completely revised and several new measurements developed. The potential of the new instruments are evident from the presented results. These tools have all the prerequisites to achieve the tight performance requirements imposed by the KLOE-2 detector in terms of injection efficiency and related background.

## REFERENCES

- [1] G. Vignola, *et al.*, Frascati Phys. Ser. **4**, 19.
- [2] A. Aloisio, *et al.*, INFN LNF preprints **92/019**.
- [3] P. Raimondi, *et al.*, physics/0702033 [PHYSICS].
- [4] C. Milardi *et al.*, J. of Instr., **7**, T03002.
- [5] A. Rizzo, *et al.*, J. Phys. Conf. Ser. **348** 012003.
- [6] C. Milardi, Int. J. Mod. Phys. **A24** 360.
- [7] M. Zobov, *et al.*, Phys. Rev. Lett. **104** 174801.
- [8] G. Amelino-Camelia, *et al.*, Eur. Phys. J. C **68** 619.
- [9] C. Milardi, *et al.* This conference (WEOCA03).
- [10] C. Milardi, *et al.* This conference (THPRI002).
- [11] “Bergoz BCM Charge Monitor User’s Manual”
- [12] A. Stecchi *et al.*, INFN-LNF Acc. Div. Internal Note, **C22**.
- [13] “Libera Brilliance User Manual”
- [14] MAD-X, <http://mad.web.cern.ch/mad/>.